Effect of Earthquake-Induced Structural Pounding on the Floor Accelerations and Floor Response Spectra of Adjacent Building Structures

PEDRO FOLHENTO[1], RUI CARNEIRO DE BARROS[2], MANUEL BRAZ-CÉSAR[3]
[1]CONSTRUCT, Faculdade de Engenharia da Universidade do Porto,
FEUP, Rua Dr. Roberto Frias, s/n 4200-465, Porto,
PORTUGAL

[2]CONSTRUCT, Faculdade de Engenharia da Universidade do Porto,
FEUP, Department of Civil Engineering – Structural Division,
Rua Dr. Roberto Frias, s/n 4200-465, Porto,
PORTUGAL

[3]CONSTRUCT, Instituto Politécnico de Bragança,
ESTiG, Campus de Santa Apolónia - 5300-253, Bragança,
PORTUGAL

Abstract: - The influence of earthquake-induced structural pounding among buildings is paramount in the seismic analysis and design of structures. The recognition of such a phenomenon has been growing in the last decades. The search for ways to understand and mitigate the consequences of these structural collisions in building structures is the primary goal of the investigation of earthquake-induced building pounding. This phenomenon is known for increasing the floor accelerations, mainly where pounding occurs, implying significant local damage. These collisions cause short-duration acceleration pulses that may compromise the building structure and the non-structural elements within the building's stories. Non-structural elements supported by the structure's floors under earthquake-induced pounding instances may present a risk to human lives and/or human activity. Hence, the influence of earthquake-induced pounding in the floor response spectra of two adjacent reinforced concrete structures with inelastic behavior is assessed by varying the number of stories and their separation distance. Pounding greatly influenced the floor acceleration spectra, increasing the spread of accelerations over a broader period range, particularly exciting low to moderate periods of vibration.

Key-Words: - Seismic analysis, Reinforced concrete structures, Building structural pounding, Non-linear inelastic behavior, Finite elements, Floor acceleration response spectrum analysis, Non-structural elements.

Received: April 17, 2023. Revised: February 19, 2024. Accepted: March 15, 2024. Published: April 23, 2024.

1 Introduction

The influence of earthquake-induced structural pounding among buildings is paramount in the seismic analysis and design of structures. This phenomenon leads to unclear patterns or trends of the colliding structure's dynamic responses, which explain contradictions in research results, [1]. The recognition of such phenomenon has grown in the last decades, contributing to a better understanding of building structural pounding and mitigation of its negative consequences, constituting the main goals in studying such occurrences in seismic events.

In this context, several mitigation measures and techniques have been proposed in the literature, [2]. Among them, the interposition of a flexible layer, bumpers, or shock absorbers between the adjacent structures, [3], [4], may reduce or soften the acceleration spikes verified in the colliding floors. Indeed, this phenomenon is known for increasing the floor accelerations, particularly where pounding occurs, implying significant local damage. Floor acceleration increases caused by pounding can reach ten times or more than the case with no pounding, [5], [6], [7], [8]. These collisions cause short-duration acceleration pulses that may compromise the building structure and the non-structural elements within the building's stories. According to Eurocode 8, [9], non-structural elements (secondary

systems) are the appendages (e.g., architectural components, mechanical or electrical equipment, partition or curtain walls, etc.) of the buildings, i.e., the building's content without a structural or load-bearing function, that in case of failure, may pose a risk to human lives and/or activity, and/or to the structure (primary system). In addition, Eurocode proposes an expression as a simplification to account for the effects of the seismic action on the structural elements. This expression comprises a parameter related to the determination of the pseudo-spectral acceleration acting on a non-structural component supported by a given floor. Such simplification would not be appropriate for essential non-structural elements, [9].

Limited studies have addressed floor spectra analysis while considering structural pounding between floors of adjacent buildings, [5], [10], [11], [12]. An investigation has considered structural collisions induced by earthquakes between buildings as multiple degrees of freedom systems to assess, among other effects, the influence of pounding on the floor accelerations and floor response spectra, [5]. The author verified significant increases in the floor accelerations due to pounding and increases in the high-frequency range of floor acceleration spectra. In another study, it was analyzed the seismic pounding retrofit of adjacent buildings, [10], verifying the effectiveness of the proposed pounding reduction devices in the high-frequency content of floor acceleration response spectra. The use of different impact models to simulate pounding forces between three adjacent building structures has been investigated, concluding that floor acceleration response spectra are sensitive to the impact model chosen, [11]. A sensitivity analysis was performed between adjacent structures considering the influence of pounding on the floor acceleration response spectra, [12]. The authors concluded that the impact impulses govern the floor response spectra in the case of severe pounding.

This paper investigates the effect of earthquake-induced structural pounding on the floor accelerations and floor response spectra of two adjacent reinforced concrete (RC) structures with variable separation distances. Pounding is considered to happen among floors, and five different configurations for the RC buildings in terms of the number of stories will be assessed. This will allow the understanding of how the different number of stories and the separation of structures may influence the non-structural elements' performance, essential for the safety of human lives and services during a seismic event causing floor collisions.

2 Problem Formulation

The present section comprises the structural and dynamic characteristics of the buildings considered in the five pounding scenarios. The choice of three recorded seismic signals adjusted to a specific seismic region also accounts for the seismic effect in the non-linear analyses.

Finally, the impact model is described to compute the pounding forces' magnitude.

2.1 Building Structures' Models

This parametric investigation is based on five scenarios of adjacent RC structures with variable separation distances, as depicted in Figure 1.

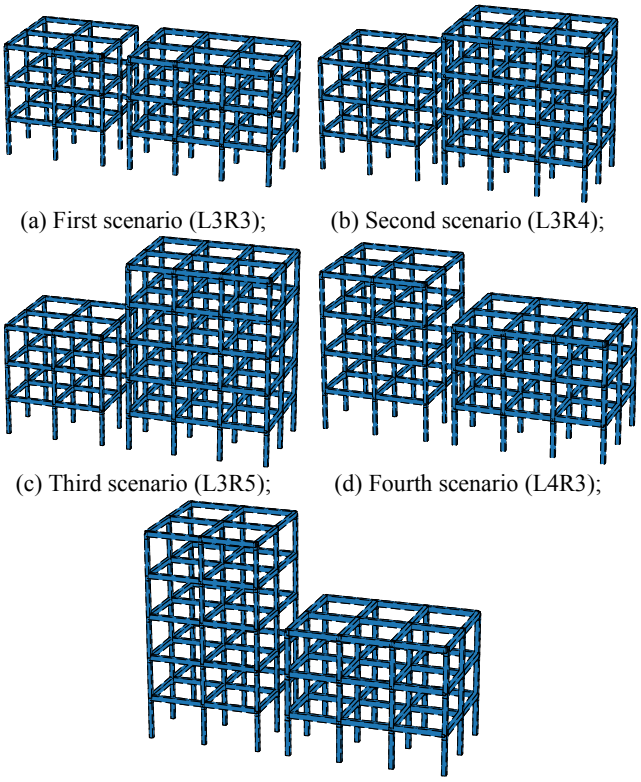

(a) First scenario (L3R3); (b) Second scenario (L3R4);

(c) Third scenario (L3R5); (d) Fourth scenario (L4R3);

(e) Fifth scenario (L5R3);

Fig. 1: Pounding scenarios of RC structures under investigation

Building 1 is always represented on the left side, while Building 2 is on the right, as shown in Figure 1 and Figure 2. The plan view of the two buildings can be seen in Figure 2. Building 1 is intended to have a more flexible layout, having structural elements with smaller cross-sections (columns 25x25cm2; beams 35x25cm^2) and slender slabs (15cm). Conversely, Building 2 has bigger cross-sections (columns: 30x30cm^2, beams 40x30cm^2) and thicker slabs (20cm). Every story has 3m of height.

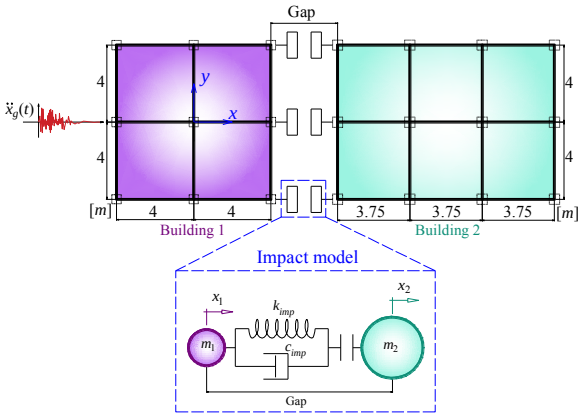

Fig. 2: Plan view of the adjacent RC building structures and the impact model

The six different fixed-base RC structures were designed according to the Eurocode, [9], [13], [14], using class C25/30 concrete and steel rebars of S500. The seismic design was performed following the weak-beam-strong-column philosophy (capacity design), considering the seismic region of Portimão, Portugal, assuming a soil type A, class of importance II, 5% damping, and medium ductility class. Second-order geometric effects are neglected in the design and analysis processes.

A live load of $2.0kN/m^2$ and $0.40kN/m^2$ was uniformly distributed over the floors and roof of the structures, respectively, [13]. Furthermore, a super dead load of $1.5kN/m^2$ was applied evenly distributed over the floors of the structures. A distributed load of $2.5kN/m$ on the exterior beams of the stories (excluding the top story) was considered to account for the mass of single-leaf exterior infill walls. Nevertheless, their additional stiffness and interaction with the main structure in the dynamic analyses are neglected for simplicity reasons.

For the calculation of the mass per story (excluding the roof) participating in the dynamic analyses, only 15% of the floor's live load is assumed. Hence, Building 1 has $56970kg$ and $48965kg$ of story and roof mass, respectively; and Building 2 has $95788kg$ and $84476kg$ of story and roof mass, respectively.

These scenarios were created from the configuration of equal heights (L3R3), varying the number of stories (3 to 5 stories) to understand how structures with unequal heights are affected by pounding. Table 1 shows the buildings' fundamental periods.

Table 1. Fundamental periods of the buildings.

Stories \ Building	1	2
3	0.5438 *s*	0.4121 *s*
4	0.7195 *s*	0.5441 *s*
5	0.8969 *s*	0.6778 *s*

The finite element numerical models are built in OpenSees, [15], using the fiber model with finite length lumped plasticity at the critical regions of plastic hinge formation (Figure 3), i.e., at the ends of the structural elements. The steel reinforcement from the design process is applied in these regions, while an elastic material is assumed at the elements' center. The constitutive laws of confined and unconfined concrete with a compressive strength of $33MPa$ and steel with a yield strength of $500MPa$ are exemplified in Figure 4.

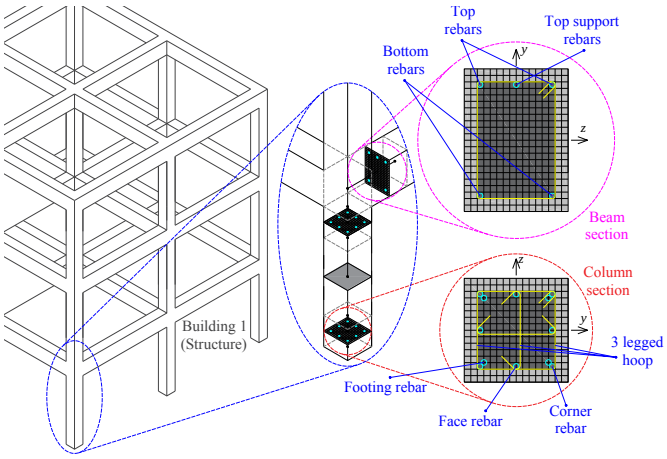

Fig. 3: Fiber model finite-length plasticity for the example of the three-story structure of Building 1

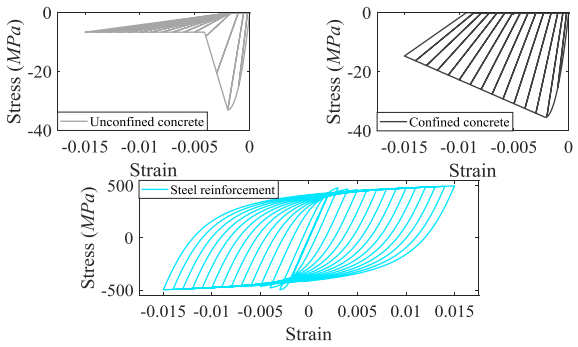

Fig. 4: Constitutive laws assumed for the materials used in the fiber model

For the concrete material, the Kent-Park-Scott model, [16], (*Concrete01*) was used, and for steel material, the Giuffré-Menegotto-Pinto model, [17], (*Steel02*).

2.2 Seismic Effect

The selection of a set of seismic signals representing the site characteristics is important to account for the variability of the seismic effect in non-linear dynamic analyses. Hence, according to Eurocode 8, a set of three recorded seismic signals, [18], is considered and adjusted to match the elastic design response spectrum of Portimão, Portugal's seismic

region, following the characteristics previously described in the design process. Table 2 shows the characteristics of the original and modified signals.

Table 2. Characteristics of the real and adjusted seismic signals considered, [19]

Name and station		*Loma Prieta, 1989 WAHO-0 RSN811*	*Northridge, 1994 ArletaNF-360 RSN949*	*El Centro, 1940 Sta9-180 RSN6*
Magnitude, *Mw*		6.93	6.69	6.95
***PGA* (m/s^2)**	Real	3.66	3.02	2.76
	Adjusted	2.39	2.82	3.00
Arias intensity (*m/s*)	Real	3.70	1.17	1.56
	Adjusted	1.20	1.81	2.58
Dominant period (*s*)	Real	0.12	0.24	0.46
	Adjusted	0.34	0.54	0.46
Significant duration (*s*)	Real	10.47	13.46	24.19
	Adjusted	10.84	21.40	24.69

Figure 5 graphically shows the adjustment of the acceleration response spectra to the above-mentioned target response spectrum.

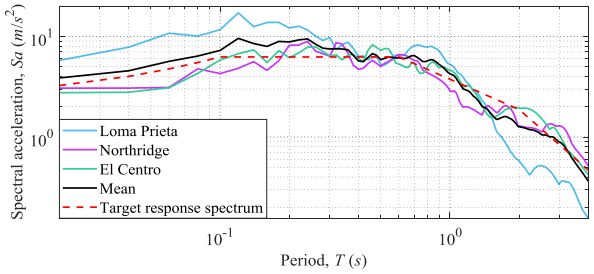

(a) Original and target response spectra;

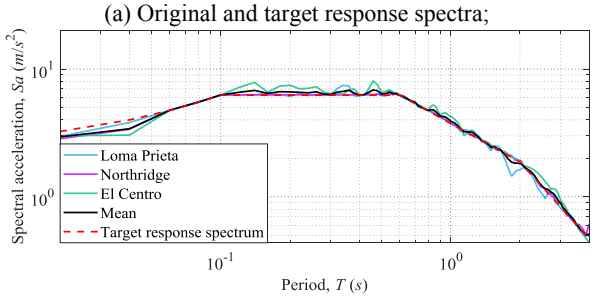

(b) Adjusted or matched and target response spectra.

Fig. 5: Response spectra adjustment

The adjustment process is carried out using the software SeismoMatch, [19], which modifies the frequency content of the accelerograms using signal processing techniques. These techniques intend to reproduce certain response spectra, viz, design response spectra.

The algorithm used by this software is based on the addition of wavelets in the time-domain acceleration signal to attain the desired spectral result adjusted to the target response spectrum, [20], [21]. Wavelet addition constitutes a correction more focused on the time domain, inducing less energy and preserving the non-stationary features of the acceleration signal, [8].

2.3 Impact Model

The pounding forces generated from the collisions between adjacent structures with different dynamic properties are calculated using the Kelvin-Voigt or linear viscoelastic impact models, [22], as represented in Figure 2.

In OpenSees, the ViscoelasticGap material, [23], is used. However, it was modified to neglect the unnatural negative pounding force verified at the end of the impacts.

Impact models are zero-length compression-only elements, constituted by a massless spring and a dashpot in parallel having thus, the advantage of being represented by fewer parameters (Impact stiffness, k_{imp}, and coefficient of restitution, CR), although their estimation may be difficult, constituting the main disadvantage of these models.

The use of these impact elements is generally based on oversimplified assumptions of the state of stress of the colliding bodies under the passage of stress waves, justifying the mass-spring-dashpot model with reasonable accuracy.

Other impact models have been recently developed by different authors, presenting great predictions of the pounding forces between buildings, [24], [25], [26], [27], [28].

The impact stiffness was assumed to be the same as the axial stiffness of the stiffer floor. The coefficient of restitution is taken as 0.65 (usual in structural applications) and was used to determine the impact damping constant, c_{imp}, as follows, [22]:

$$c_{imp} = 2\,\xi_{imp}\sqrt{k_{imp}\frac{m_1 m_2}{m_1 + m_2}} \qquad \text{where } \xi_{imp} = \frac{-\ln(CR)}{\sqrt{\pi^2 + \left[\ln(CR)\right]^2}} \tag{1}$$

In which m_i is the lumped mass of one story of a Building i, and ξ_{imp} is the impact damping ratio. These parameters are then included in the piecewise function that computes the pounding force depending on the interpenetration depth δ (=x_1-x_2-Gap), the condition of impact,

$$f_P(t) = \begin{cases} k_{imp}\,\delta(t) + c_{imp}\,\dot{\delta}(t), & \text{for } \delta(t) > 0 \\ 0 & \text{for } \delta(t) \le 0 \end{cases} \tag{2}$$

A relatively small time step must be undertaken to capture an impact between adjacent building structures. However, very small time steps condition the feasibility of parametric studies since these are incompatible with computationally demanding simulations. To address this, a condition of

proximity was included in the non-linear dynamic time history analyses. A fraction of the gap size triggers this condition of proximity of the adjacent buildings. The normal time step was assumed to be 5×10^{-3} *s*, and when a collision is approaching or happening, the time step is reduced to 2×10^{-4} *s*.

The simulation time is considerably reduced, and the accuracy in capturing and calculating the pounding forces is maintained. Still, care should be taken for discrepancies between these time steps, which may lead to convergence problems.

3 Results and Discussion

A series of non-linear time-history analyses were carried out.

The results of these analyses will be presented and discussed in terms of the number and magnitude of collisions, floor accelerations, and floor response spectra for the five pounding scenarios considered and across all the values considered for the gap size or separation distance.

The gap size values were assumed to vary between the nearly zero gap (5 *mm*, here referred to as "zero-gap") until no collisions were verified.

3.1 Number and Magnitude of Pounding Forces

Figure 6 presents the number of impacts verified for the three adjusted seismic signals and pounding scenarios over the gap sizes considered. Similarly, Figure 7 shows the results regarding the magnitude of pounding forces.

The number of collisions and their magnitude naturally depends on the separation distance. Nevertheless, a zero-gap size does not always present the highest magnitude of pounding force, though it is always the case with a greater number of impacts.

A scenario that presents a greater difference in the number of stories will be more susceptible to more collisions and of a larger magnitude than a scenario with an equal number of stories and the same height. In particular, scenario L5R3, an RC structure with a more flexible layout and a greater number of stories (L5) than the adjacent structure that has a stiffer structural configuration and fewer stories (R3), performs worse than the opposite scenario, L3R5.

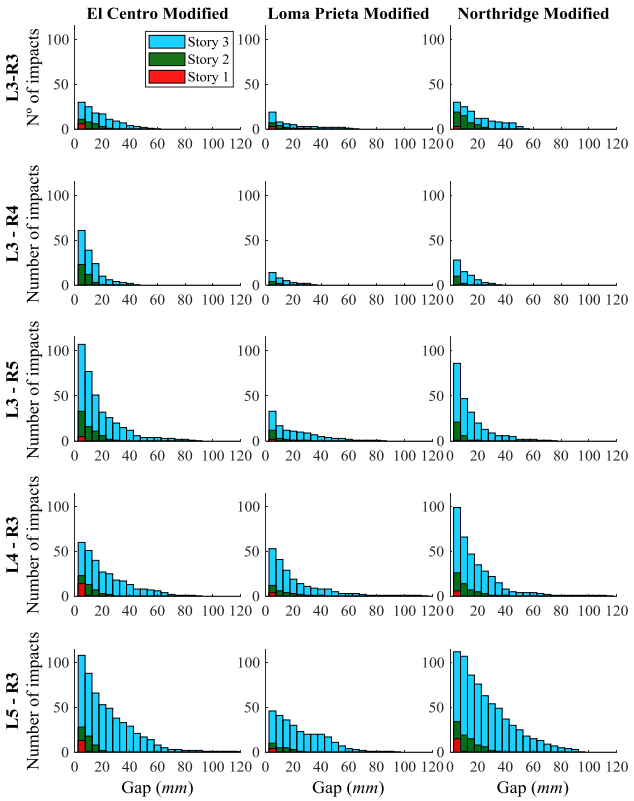

Fig. 6: Number of impacts per story for the different scenarios studied

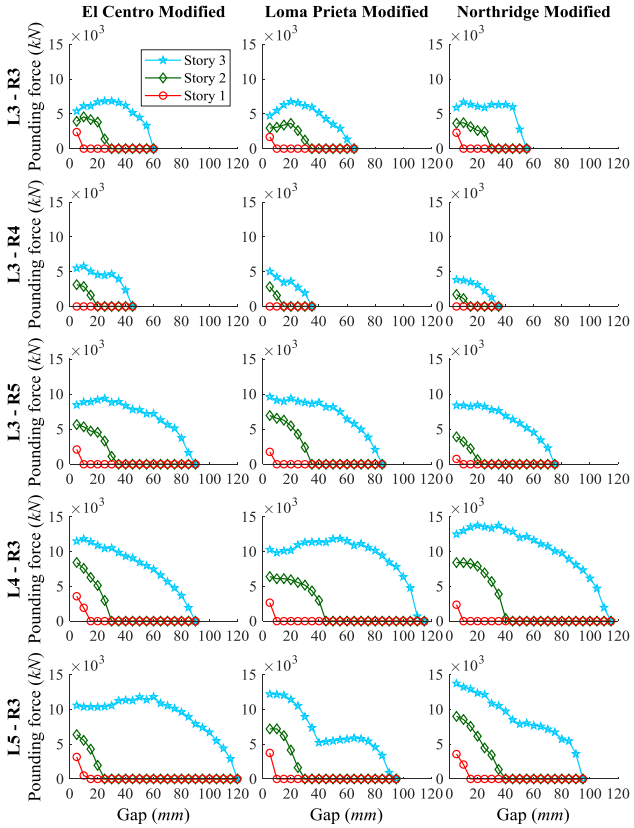

Fig. 7: Maximum pounding force per story for the different scenarios studied

The top story consistently exhibits the highest magnitude and number of collisions since it experiences the largest relative displacements.

The number of impacts decreases significantly with the increase of the gap size. The magnitude of the pounding forces also decreases with the increasing gap size. However, it is not as evident as with the number of impacts.

Overall, the adjusted seismic signals tend to present a similar trend with gap size variation. Loma Prieta earthquake shows a smaller number and magnitude of impacts, due to the reduced duration and different dominant periods of vibration (Table 2).

Figure 8 presents the case with the biggest number of collisions and higher magnitude of the pounding force. Figure 9 shows the first scenario that presents the highest magnitude of pounding force. Moreover, Figure 10 shows the pounding cycles, typical of the Kelvin-Voigt impact model without the tensile force, corresponding to Figure 8 and Figure 9.

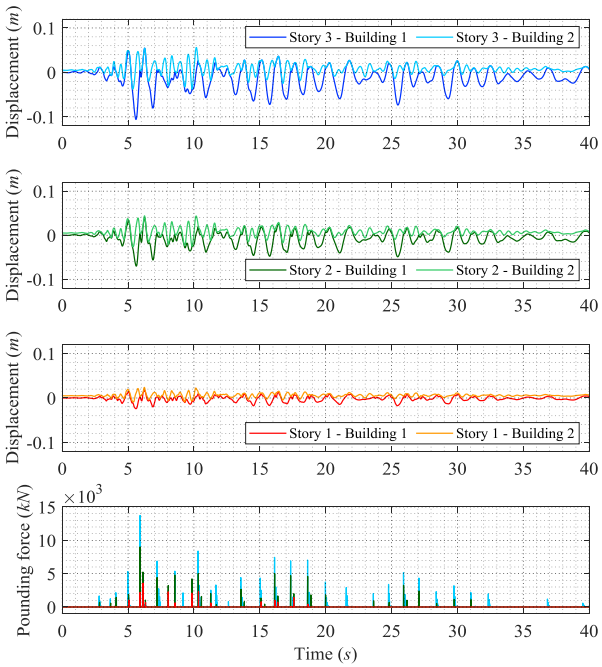

Fig. 8: Displacements and pounding forces time history of the colliding stories in scenario L5R3 with zero-gap size under the modified Northridge earthquake

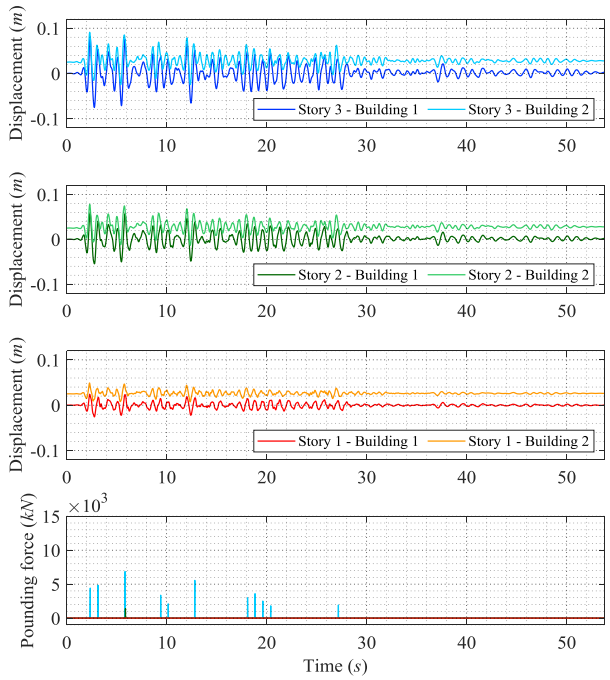

Fig. 9: Displacements and pounding forces time history of the colliding stories in scenario L3R3 with 2.5 *cm* of gap size under the modified El Centro earthquake

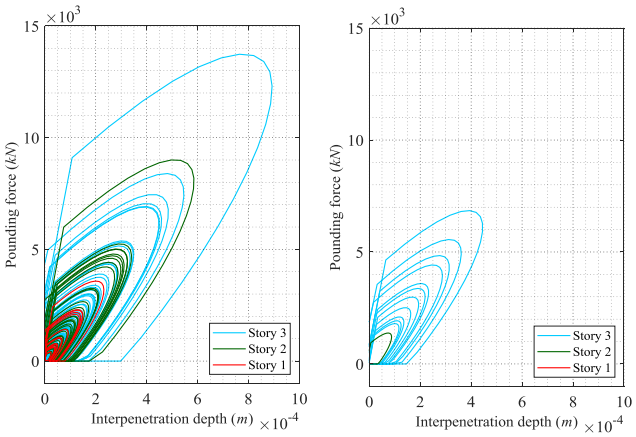

Fig. 10: Pounding cycles of the cases presented in Figure 8 and Figure 9, respectively

These collisions are thus associated with a steep variation of the adjacent buildings' velocity corresponding to acceleration spikes, to which significant local damage is implied.

The following two subsections will address how these acceleration spikes influence each structure and non-structural elements supported by the floors.

3.2 Floor Accelerations

The acceleration spikes' values are proportional to the pounding forces' values, as seen in the comparison of Figure 9 and Figure 11. Hence, the same conclusions regarding the gap sizes can be derived from the previous sub-sections. Figure 11

and Figure 12 present examples of the floor acceleration time histories in two of the scenarios studied. In these figures, it is possible to witness the sudden increases in acceleration due to building pounding. A zero-gap size scenario will present a higher number of acceleration spikes, and of significant amplitude, constituting one of the worst scenarios in pounding.

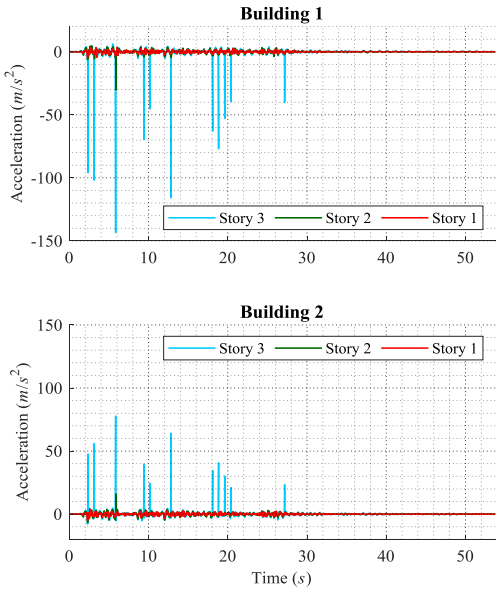

Fig. 11: Acceleration time-histories for the first scenario with a 2.5 *cm* gap size under the modified El Centro earthquake

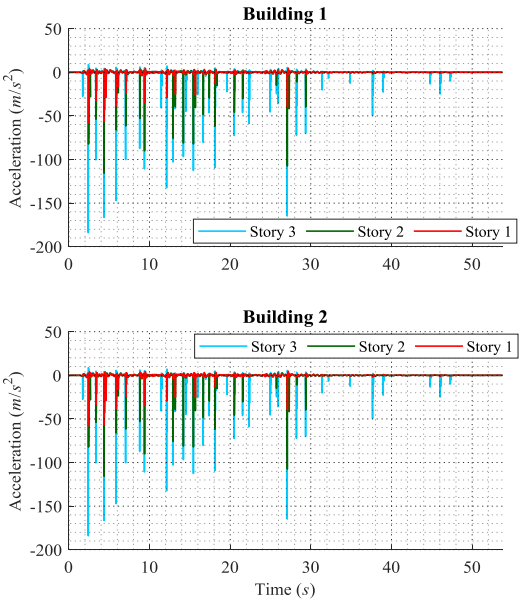

Fig. 12: Acceleration time-histories for the last scenario with zero-gap size under the modified El Centro earthquake

Figure 13, Figure 14, Figure 15, Figure 16 and Figure 17 present the maximum absolute acceleration ratio between the case with and without pounding for every scenario under the modified El Centro earthquake and for some of the gap sizes.

Conclusions, however, will be reflected for every seismic signal studied and gap size. The positive and negative signs reflect the inbound and rebound directions of each building, as can be confirmed by Figure 8, Figure 9, Figure 11 and Figure 12, e.g., a negative acceleration in Building 1 corresponds to its rebound direction.

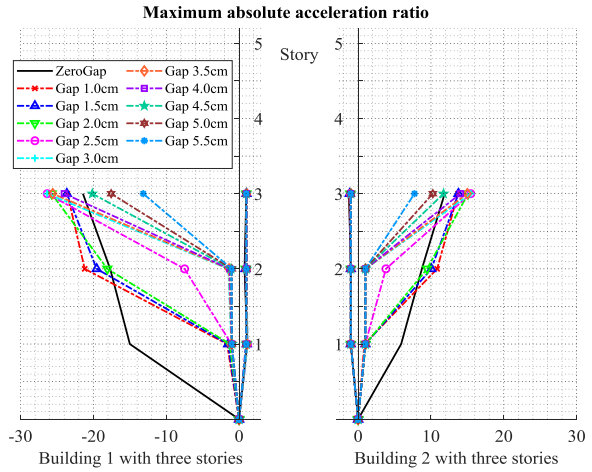

Fig. 13: Maximum absolute acceleration ratios for the first scenario under the modified El Centro earthquake

Results from every seismic signal show that absolute accelerations can suffer sudden and momentary increases due to pounding forces that can achieve 80 times those without collisions.

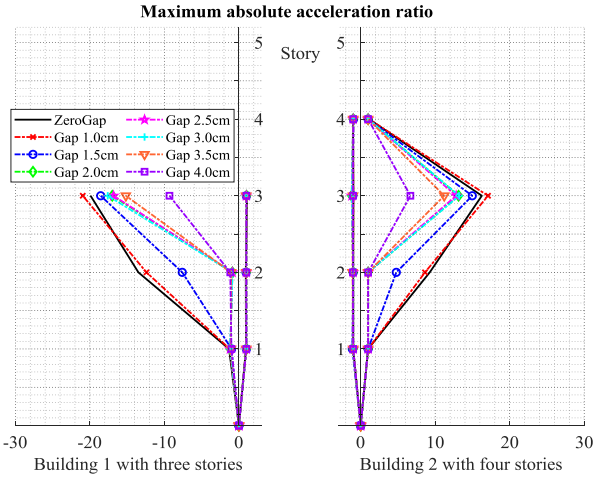

Fig. 14: Maximum absolute acceleration ratios for the second scenario under the modified El Centro earthquake.

The absolute acceleration ratios reveal that Building 1, possessing the most flexible layout, is

significantly more vulnerable to pounding forces. Building 1 presents increases in the maximum absolute acceleration concerning the case without pounding that are higher (scenarios L3R3, L3R4, L4R3, and L5R3) or approximately equal (L3R5) to the ones verified in Building 2.

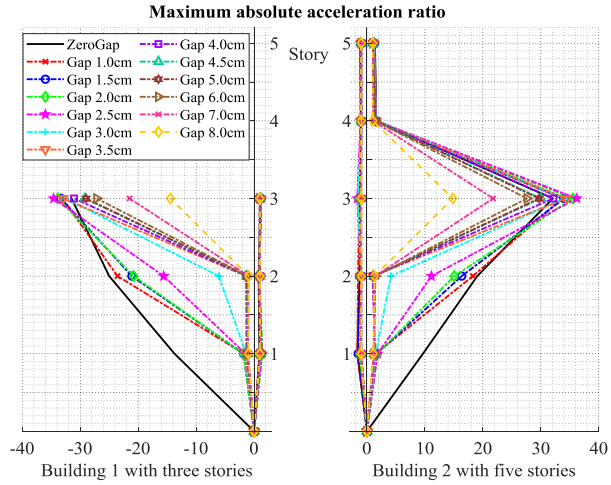

Fig. 15: Maximum absolute acceleration ratios for the third scenario under the modified El Centro earthquake

Accelerations are significantly affected in the stories where pounding occurs and have little influence in the stories without pounding, evident when buildings have unequal heights (Figure 14, Figure 15, Figure 16 and Figure 17).

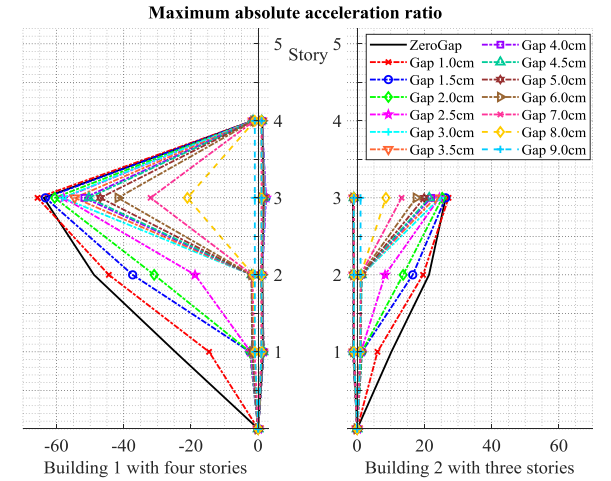

Fig. 16: Maximum absolute acceleration ratios for the fourth scenario under the modified El Centro earthquake

The scenarios related to pounding between buildings with different numbers of stories show higher increases in absolute acceleration compared with the L3R3 scenario. The exception is scenario L3R4, which presents the smallest increases in absolute accelerations compared with the cases without pounding. This is justified by the observation of the fundamental periods of the structures (Table 1) that are nearly identical, producing an almost in-phase response, which also explains the reduced magnitude and number of impacts (Figure 6 and Figure 7).

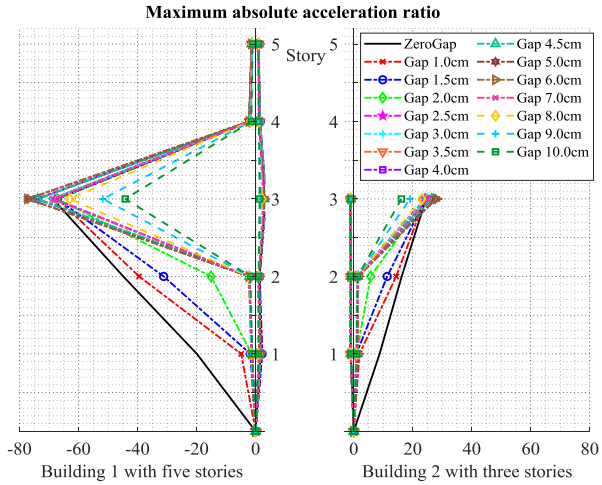

Fig. 17: Maximum absolute acceleration ratios for the fifth scenario under the modified El Centro earthquake

Regarding the effect of gap sizes, generally for the different ground motions, one can verify that the smallest separation distances do not always result in the highest increases (Gap 2.5 – 6.0 *cm*) in absolute acceleration, as can be verified in the scenarios where the difference in the number of stories is greater (scenarios L3R5 and L5R3).

Similar results were obtained among the seismic signals. However, the El Centro earthquake generally provided higher increases in story absolute accelerations over a wider gap size range.

3.3 Floor Acceleration Response Spectra

The floor acceleration response spectra, or just floor response spectra, are now derived for the different scenarios, gap sizes, and ground motions mentioned previously.

In addition to the threat to human lives and activity, damage to non-structural elements during seismic events may result in substantial economic losses.

Several non-linear time-history analyses were performed to assess the influence of pounding forces in the adjacent building structures' floor acceleration response spectra. The process undertaken is now explained in the following paragraphs, and conclusions are then withdrawn based on the observation of graphic results.

Following the non-linear time-history analyses, the accelerations of the various floors of the primary structures (Buildings 1 and 2) are computed and recorded. A non-structural component is now considered (the secondary element) as a single degree of freedom (SDOF), supported by a floor of the primary structure and characterized by a period of vibration and a damping ratio. By subjecting the SDOF component to a certain floor acceleration for different values of the period of vibration and recording the maximum acceleration value, the floor acceleration response spectrum can be constructed. The seismic demand of a non-structural element on a certain floor is now known, assuming that the dynamic interaction between the primary and secondary components is insignificant.

The period of vibration is varied over a range of values suitable to the structural and non-structural components applications, and a damping ratio of 5% is assumed.

Many factors influence the floor acceleration response of building structures, viz., the structural system, the building's height, the fundamental period of vibration of the structure, the dominant period of the earthquake excitation, damping, inelastic behavior, etc. [29]. Structural pounding between adjacent buildings is another factor that significantly influences the floor response spectra.

Figure 18 shows the comparison of the floor response spectra for the first scenario without pounding under the modified El Centro earthquake, revealing the influence of the structures' inelastic behavior. Inelastic behavior tends to increase the dominant period of the structures' stories, particularly true for the upper stories. In addition, it reduces the magnitude of accelerations.

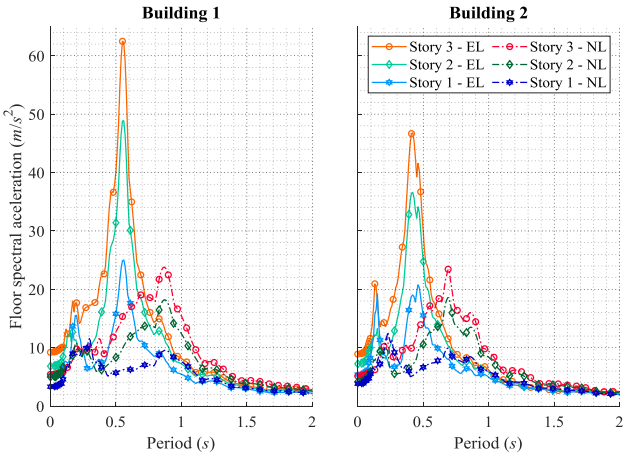

Fig. 18: Comparison of response spectra

Since the earthquake signals were adjusted to a seismic region and the seismic effect was not significant, the mean floor response spectra of the three ground motions were obtained for the different scenarios, and for most of the gap sizes considered. The mean floor acceleration response spectra were obtained for different gap sizes, accounting for pounding until the gap size, where the absence of pounding was verified. Figure 19, Figure 20, Figure 21, Figure 22 and Figure 23 show the graphic results in a logarithmic scale.

The first and foremost conclusion that can be withdrawn is the evident and expected increase of story accelerations for higher modes (smaller periods of vibration) due to pounding. This increase becomes more pronounced for smaller gap sizes, and as concluded in the previous results, the zero-gap size is not always the worst-case scenario. Depending on the scenario, gap sizes between 1 and 3 *cm* provided higher accelerations than the zero-gap size (second and third stories of L3R3 and third stories of L5R3).

Building pounding slightly reduced the magnitude of floor accelerations for moderate, but especially larger periods (from 0.5*s* and 1.0*s*), more evident in Building 1 in scenarios L3R5, L4R3, and L5R3.

Non-structural elements in the colliding stories characterized by higher frequencies or low periods (mostly in periods between 0.01*s* and 0.25*s*) will thus be very susceptible to events of structural pounding, particularly true for scenarios in which Building 1 is the tallest structure.

The shape of the floor acceleration response spectra is completely changed in the range of low periods when pounding occurs. Not only the stories under impacts are affected, but the stories above are also influenced by acceleration rises of twice the magnitude of the case without pounding (fourth story of scenarios L3R5 and L4R3, and the fourth and fifth stories of scenario L5R3). For the same reasons explained in the previous subsection, scenario L3R4 leads to a phase synchronization of both buildings, resulting in only a slight influence in the stories above and below the collisions. However, substantial increases in floor acceleration at the colliding stories are still verified.

Scenarios in which the buildings have different numbers of stories generally presented higher floor accelerations across the various gap sizes considered. The gap size plays a vital role in the floor response spectra. An adequate separation distance may reduce substantially the floor accelerations and hence reduce damage. Nevertheless, a gap size close to the no-pounding case still presented high floor accelerations on the colliding stories that are susceptible to causing

damage to non-structural components, e.g., the gap size of 9*cm* in the third to fifth scenarios.

Comparing the floor response spectra between the two building structures, one can verify that a building with a more flexible layout (Building 1) will be more susceptible to pounding instances than a structure with a stiffer layout (Building 2).

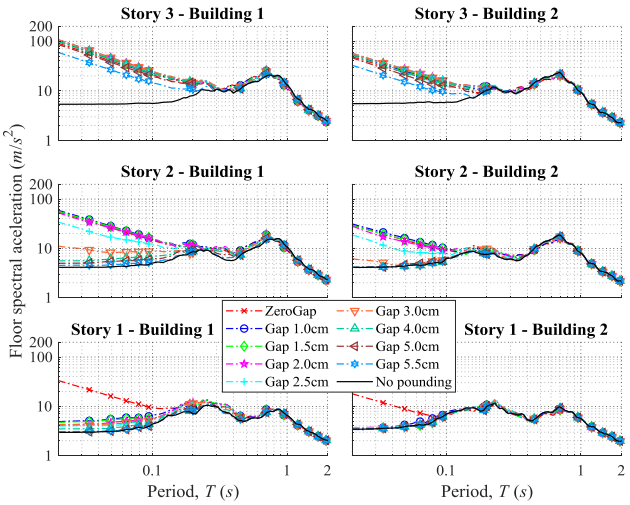

Fig. 19: Floor response spectra of the first scenario (L3R3) for different gap sizes

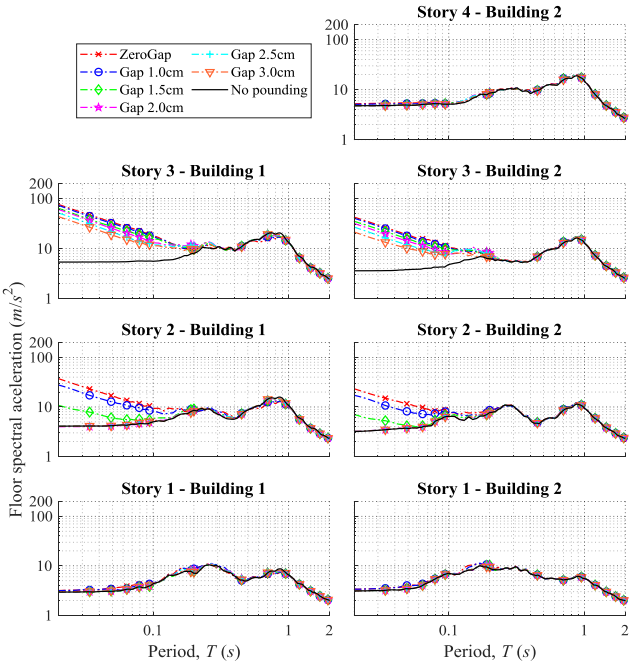

Fig. 20: Floor response spectra of the second scenario (L3R4) for different gap sizes

This can be verified by comparing the two buildings in the first scenario (Figure 19) and the opposite scenarios of an unequal number of stories, i.e., L3R4 with L4R3 (Figure 20 and Figure 22), and L3R5 with L5R3 (Figure 21 and Figure 23).

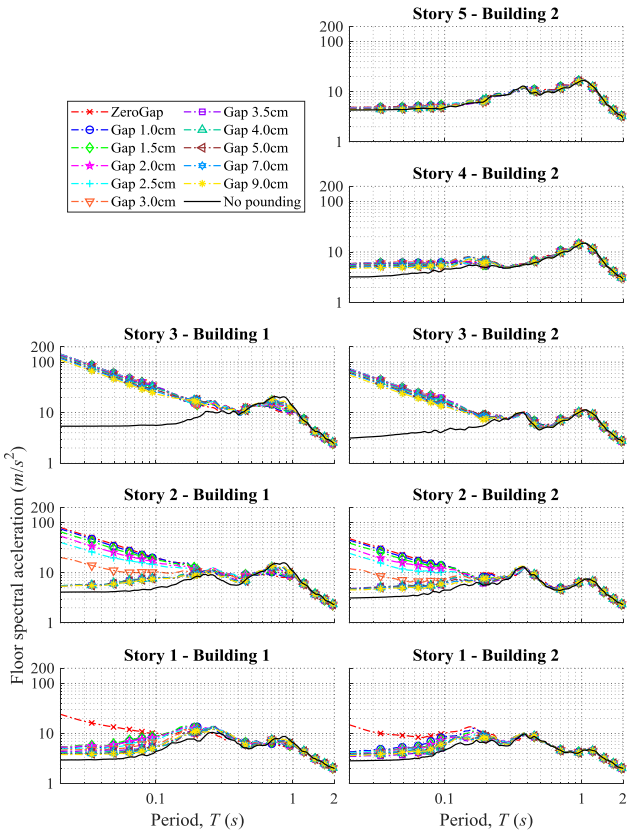

Fig. 21: Floor response spectra of the third scenario (L3R5) for different gap sizes

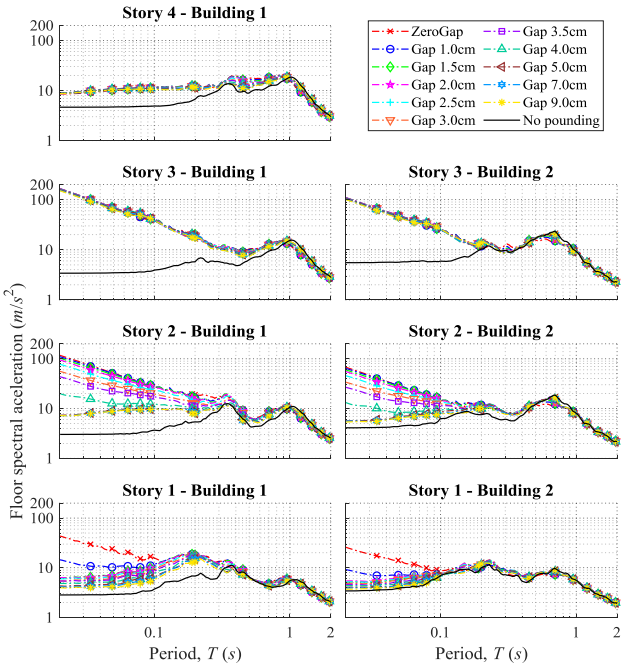

Fig. 22: Floor response spectra of the fourth scenario (L4R3) for different gap sizes

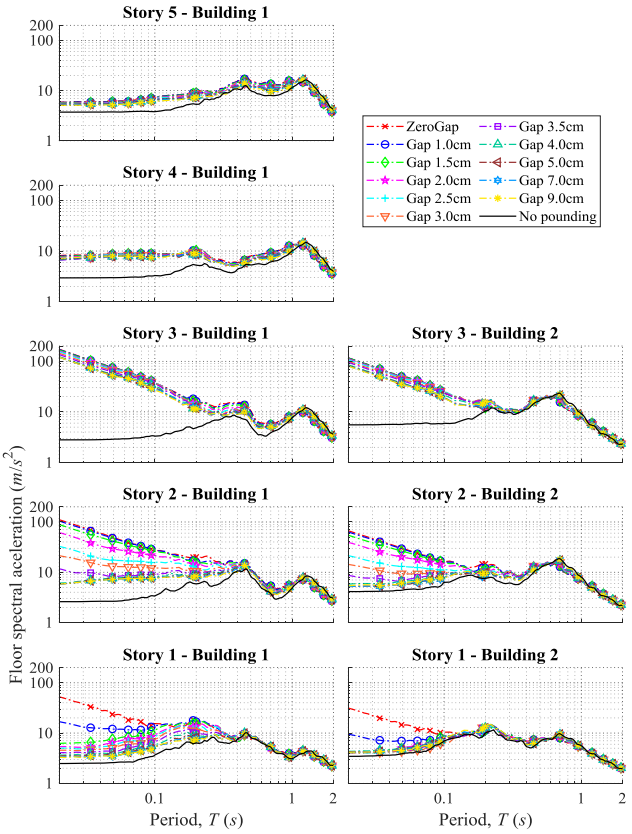

Fig. 23: Floor response spectra of the fifth scenario (L5R3) for different gap sizes

Building 1 will be more vulnerable to pounding, presenting increases in the floor acceleration for a wider range of periods of vibration (low to moderate periods), as can be verified in scenarios L4R3 and L5R3.

4 Conclusion

The present study investigated the influence of earthquake-induced structural pounding on the floor accelerations and floor acceleration response spectra of two building structures with a varying number of stories and separation distances. Different scenarios were derived based on the number of stories. It was verified that adjacent buildings with a different number of stories led to a higher number and magnitude of pounding forces, which will influence their floor acceleration response significantly. It was observed that the peak absolute acceleration suffered sudden increases due to pounding forces of approximately 80 times the peak acceleration without pounding. Pounding forces significantly altered the shape of the floor response spectra in the low period range (between 0.01*s* and 0.2*s*). Substantial damage in non-structural elements may thus be expected, particularly in the colliding stories. Building 1, characterized by a more flexible layout than Building 2, was more vulnerable to pounding forces, revealing increases in floor acceleration for a broader range of periods of vibration (low to moderate periods). Generally, a very small gap size or no separation distance led to the highest increases in floor accelerations due to pounding. Although a gap size close to the case without pounding offered similar results to the smaller gap sizes in some cases, since only one collision may generate a sudden acceleration response of the buildings' stories.

Hence, buildings adjacent to smaller structures presenting a stiffer structural layout can be particularly vulnerable to earthquake-induced structural pounding. Non-structural elements supported by colliding stories in these conditions must be carefully designed to withstand sudden and large acceleration spikes.

Future studies should address additional pounding scenarios, i.e., more variations of the number of stories, pounding between floors and columns, and the consideration of more ground excitations, assessing both near-field and far-field ground motions. Further developments and directions will also include the assessment of floor accelerations and floor response spectra in the case of adjacent buildings equipped with solutions to mitigate earthquake-induced structural pounding, such as rubber bumpers and/or passive and semi-active vibration control devices.

Acknowledgments:
This paper is within the scope of the first author's Ph.D. degree in progress, financially supported by the Portuguese Foundation for Science and Technology (FCT) through the PhD grant reference SFRH/BD/139570/2018, finished in April 2023, under the program POCH (N2020 – P2020) and subsidized by the European Social Fund (FSE) and national funds from MCTES. This work was financially supported by: Base Funding - UIDB/04708/2020 with DOI: 10.54499/UIDB/04708/2020 (https://doi.org/10.54499/UIDB/04708/2020) of the CONSTRUCT - Instituto de I&D em Estruturas e Construções - funded by national funds through the FCT/MCTES (PIDDAC).

References:

[1] M. Mahmoud, K. Choong, R. Jankowski, Seismic pounding between adjacent buildings: Identification of parameters, soil interaction issues and mitigation measures, *Soil*

Dynamics and Earthquake Engineering, Vol.121, No.2019, 2019, pp. 135-150, https://doi.org/10.1016/j.soildyn.2019.02.024.

[2] P. Folhento, R. Barros, M. Braz-César, Mitigation of Earthquake-Induced Structural Pounding Between Adjoining Buildings – State-of-the-Art, In: Gonçalves, J.A., Braz-César, M., Coelho, J.P. (eds) CONTROLO 2020. CONTROLO 2020. *Lecture Notes in Electrical Engineering*, vol 695. Springer, Cham, https://doi.org/10.1007/978-3-030-58653-9_72.

[3] P. Polycarpou, P. Komodromos, A. Polycarpou, A nonlinear impact model for simulating the use of rubber shock absorbers for mitigating the effects of structural pounding during, *Earthquake Engineering and Structural Dynamics*, Vol.42, 2013, pp. 81-100, https://doi.org/10.1002/eqe.2194.

[4] S. Khatami, H. Naderpour, S. Razavi, R. Barros, A. Jakubczyk-Gałczyńska, R. Jankowski, Study on Methods to Control Interstory Deflections, *Geosciences*, Vol.10, No.2, 2020, 75, https://doi.org/10.3390/geosciences10020075.

[5] M. Rohanimanesh, Mutual pounding of structures during strong earthquakes, *Dissertation*, *Virginia Polytechnic Institute and State University*, 1994.

[6] M. Jameel, A. Islam, R. Hussain, S. Hasan, Khaleel, Non-linear FEM analysis of seismic induced pounding between neighbouring multi-storey structures, *Latin American Journal of Solids and Structures*, Vol.10, No.5, 2013, pp. 921-939, https://doi.org/10.1590/S1679-78252013000500004.

[7] S. Raheem, M. Fooly, A. Shafy, Y. Abbas, M. Omar, M. Latif, S. Mahmoud, Seismic Pounding Effects on Adjacent Buildings in Series with Different Alignment Configurations, *Steel and Composite Structures*, Vol.28, No.3, 2018, pp. 289-308, https://doi.org/10.12989/scs.2018.28.3.289.

[8] S. Raheem, M. Fooly, A. Shafy, A. Taha, Y. Abbas, e M. Latif, Numerical simulation of potential seismic pounding among adjacent buildings in series, *Bulletin of Earthquake Engineering*, Vol.17, pp. 439-471, 2019, https://doi.org/10.1007/s10518-018-0455-0.

[9] European Committee for Standardization (ECS), Eurocode 8 (EC8): Design of structures for earthquake resistance – Part 1: General rules, seismic actions and rules for buildings (EN 1998-1), Brussels, Belgium, 2004, [Online]. https://www.phd.eng.br/wp-content/uploads/2015/02/en.1998.1.2004.pdf (Accessed Date: April 22, 2024).

[10] F. Lavelle, R. Sues, Seismic pounding retrofits for closely spaced buildings, *In Earthquake Engineering, Tenth World Conference*, Balkema, Rotterdam, 1992.

[11] N. Mate, S. Bakre, and O. Jaiswal, Seismic pounding of adjacent linear elastic buildings with various contact mechanisms for impact simulation, *Asian Journal of Civil Engineering (BHRC)*, Vol.16, No.3, 2015, pp. 383-415.

[12] V. Crozet, I. Politopoulos, M. Yang, J.-M. Martinez, S. Erlicher, Sensitivity analysis of pounding between adjacent structures, *Earthquake Engineering and Structural Dynamics*, Vol.47, No.1, 2018, pp. 219-235, https://doi.org/10.1002/eqe.2949.

[13] European Committee for Standardization (ECS), Eurocode 1 (EC1), EN 1991-1-1: Actions on structures - Part 1-1: General actions - Densities, self-weight, imposed loads for buildings, Brussels, Belgium, 2002, [Online]. https://www.phd.eng.br/wp-content/uploads/2015/12/en.1991.1.1.2002.pdf (Accessed Date: April 22, 2024).

[14] European Committee for Standardization (ECS), Eurocode 2 (EC2), EN 1992-1-1: Design of concrete structures - Part 1-1: General rules and rules for buildings, Brussels, Belgium, 2004, [Online]. https://www.phd.eng.br/wp-content/uploads/2015/12/en.1992.1.1.2004.pdf (Accessed Date: April 22, 2024).

[15] F. McKenna, OpenSees: A framework for earthquake engineering simulation, *Computing in Science & Engineering*, Vol.13, No.4, 2011, pp. 58-66, https://doi.org/10.1109/MCSE.2011.66.

[16] B. Scott, R. Park, M. Priestley, Stress-strain behavior of concrete confined by overlapping hoops at low and high strain rates. ACI Journal Proceedings, Vol.79, No.1, 1982, pp. 13-27, https://doi.org/10.14359/10875.

[17] F. Filippou, E. Popov, V. Bertero, Effects of Bond Deterioration on Hysteretic Behavior of Reinforced Concrete Joints, *Report EERC 83-19, Earthquake Engineering Research Center, University of California, Berkeley*, 1983.

[18] Pacific Earthquake Engineering Research Center (PEER) strong ground motion data base, [Online]. https://peer.berkeley.edu/peer-strong-ground-motion-databases (Accessed Date: February 15, 2024).

[19] Seismosoft (2021). SeismoMatch version 2021, [Online]. http://www.seismosoft.com (Accessed Date: February 15, 2024).

[20] N. Abrahamson, Non-stationary spectral matching, *Seismological Research Letters*, Vol.63, No.1, 1992, pp. 30.

[21] J. Hancock, J. Watson-Lamprey, N. Abrahamson, J. Bommer, A. Markatis, E. McCoy, R. Mendis, An improved method of matching response spectra of recorded earthquake ground motion using wavelets, *Journal of Earthquake Engineering*, Vol.10, No.S1, 2006, pp. 67-89, https://doi.org/10.1080/13632460609350629.

[22] S. Anagnostopoulos, Equivalent viscous damping for modeling inelastic impacts in earthquake pounding problems, *Earthquake Engineering and Structural Dynamics*, Vol.33, No.8, 2004, pp. 897-902, https://doi.org/10.1002/eqe.377.

[23] P. Hughes, G. Mosqueda, Evaluation of uniaxial contact models for moat wall pounding simulations, *Earthquake Engineering and Structural Dynamics*, Vol.49, No.12, 2020, pp. 1197-1215, https://doi.org/10.1002/eqe.3285.

[24] H. Naderpour, R. Barros, and S. Khatami, A new model for calculating impact force and energy dissipation based on the CR-factor and impact velocity, *Scientia Iranica A*, vol. 22, 2015, pp. 59-68.

[25] F. Bamer, A Hertz-pounding formulation with a nonlinear damping and a dry friction element, *Acta Mechanica*, vol. 229, 2018, pp. 4485-4494, https://doi.org/10.1007/s00707-018-2233-0.

[26] F. Bamer and B. Markert, A nonlinear visco-elastoplastic model for structural pounding, *Earthquake Engineering, and Structural Dynamics*, vol. 47(12), 2018, pp. 2490-2495, https://doi.org/10.1002/eqe.3095.

[27] F. Bamer, N. Strubel, J. Shi and B. Markert, A visco-elastoplastic pounding damage formulation, *Engineering Structures*, vol. 197, 2019, https://doi.org/10.1016/j.engstruct.2019.109373.

[28] S. Khatami, H. Naderpour, R. Barros, A. Jakubczyk-Gałczynska and R. Jankowski, Effective Formula for Impact Damping Ratio for Simulation of Earthquake-induced Structural Pounding, *Geosciences*, Vol.9, No.8, 2019, 347, https://doi.org/10.3390/geosciences9080347.

[29] C. Murty, R. Goswami, A. Vijayanarayanan, R. Kumar, V. Mehta, Introduction to Earthquake Protection of Non-structural Elements in Buildings, *Gujarat State Disaster Management Authority*, Government of Gujarat, 2012.

Contribution of Individual Authors to the Creation of a Scientific Article (Ghostwriting Policy)

The authors equally contributed in the present research, at all stages from the formulation of the problem to the final findings and solution.

Sources of Funding for Research Presented in a Scientific Article or Scientific Article Itself

This paper is within the scope of the first author's Ph.D. degree in progress, financially supported by the Portuguese Foundation for Science and Technology (FCT) through the PhD grant reference SFRH/BD/139570/2018, finished in April 2023, under the program POCH (N2020 – P2020) and subsidized by the European Social Fund (FSE) and national funds from MCTES. This work was financially supported by: Base Funding - UIDB/04708/2020 with DOI: 10.54499/UIDB/04708/2020 (https://doi.org/10.54499/UIDB/04708/2020) of the CONSTRUCT - Instituto de I&D em Estruturas e Construções - funded by national funds through the FCT/MCTES (PIDDAC).

Conflict of Interest

The authors have no conflicts of interest to declare.